MS.ID-IJPBS-1311
International Journal of Pharmacy and Biological Sciences-IJPBS™ (2025) 15 (4): 91-115
Online ISSN: 2230-7605, Print ISSN: 2321-3272
Research Article | Pharmaceutical Sciences | OA Journal | MCI Approved | Index Copernicus

Modulation Of Beclin-1 and Bcl-2 Expression by Intermittent Fasting In CRC: Links to Autophagy and Apoptosis

K Pavan Kumar[1] * and Amit Kumar[2]

[1]Research Scholar, Faculty of Pharmaceutical Sciences, Motherhood University Dehradun Road, Karoundi Village, Bhagwanpur Post, Roorkee Tehsil, Haridwar Distt., Uttarakhand-247661.

[2]Professor, Faculty of Pharmaceutical Sciences, Motherhood University Dehradun Road, Karoundi Village, Bhagwanpur Post, Roorkee Tehsil, Haridwar Distt., Uttarakhand-247661.

Received: 29 May 2025/ Accepted: 2 Jun 2025 / Published online: 17 Nov 2025
***Corresponding Author Email:** fops.pavan@motherhooduniversity.edu.in

Abstract

Colorectal cancer (CRC) represents a leading cause of cancer-related morbidity and mortality worldwide, driven by the dysregulation of signaling pathways controlling autophagy and apoptosis. The present study investigates the mechanistic influence of intermittent fasting (IF) on the modulation of Beclin-1 and Bcl-2—key regulators linking autophagy and apoptosis—in a colorectal cancer rat model. Experimental animals were divided into seven groups, including controls, fasting durations (6, 12, 18, and 24 hours), and a standard drug treatment group. Aberrant crypt foci (ACF) quantification, histopathology, immunohistochemistry, TUNEL assay, Western blotting, ELISA, qRT-PCR, and molecular analyses were performed to evaluate the effects of IF on cellular and biochemical markers. IF induced a time-dependent modulation of Beclin-1 and Bcl-2 expression, with 24-hour fasting showing the highest expression intensity. Significant reductions in pro-inflammatory proteins (NF-κB, TNF-α, IL-6) and oxidative stress markers were observed, accompanied by restoration of antioxidant enzymes (SOD, CAT, GSH, GPx) and normalization of Caspase-3 activity. These findings demonstrate that intermittent fasting enhances autophagic clearance and sensitizes tumor cells to apoptosis by rebalancing Beclin-1/Bcl-2 signaling and reducing inflammatory stress. Thus, IF may serve as a promising metabolic intervention for colorectal cancer prevention and adjunct therapy by targeting molecular crosstalk between autophagy and apoptosis.

Keywords

Embinin, Colorectal Cancer, Aberrant crypt foci, histopathology, immunohistochemistry, TUNEL assay, Western blotting, ELISA, qRT-PCR etc.

*****

INTRODUCTION

Colorectal cancer is a complex and multifactorial disease that involves dysregulation of multiple signaling pathways (Arnold et al., 2017). Among these pathways, autophagy and apoptosis constitute the two major events of the tumorigenesis (Levy et al., 2017). Since both these pathways are involved in maintaining cellular homeostasis under a number of unphysiological conditions, in order to characterize these pathways as therapeutic targets in cancer

pathogenesis, there is a need to delineate the context dependent intricate interplay between autophagy and apoptosis in suitable tumor models (Mariño et al., 2014).

The term "autophagy" typically refers to the macro-autophagy which is a dynamic process involved in the degradation of cytoplasmic proteins and organelles through the lysosomal pathway (Mizushima & Komatsu, 2011). This process is regulated by a set of highly conserved genes known as autophagy-related genes (ATG) (Yang & Klionsky, 2020). Apoptosis, a type I category programmed cell death (PCD I), is a tightly regulated physiological process that autonomously triggers cell death (Elmore, 2007). It is characterized by distinct cellular changes, including cell shrinkage, membrane blebbing, DNA fragmentation, and the formation of apoptotic bodies (Kerr et al., 1972). The apoptotic process involves exogenous or death receptor mediated and the intrinsic or mitochondrial pathways (Tait & Green, 2010; Taylor et al., 2008; Galluzzi et al., 2018). The interplay between autophagy and apoptosis are critical in the development of tumors (Mariño et al., 2014). Various studies have suggested that there is a reciprocal relationship between autophagy and apoptosis which is regulated by shared signal transduction pathways and factors like Beclin1, Bcl-2, caspases, and p62 (Maiuri et al., 2007; Pattingre et al., 2005).

Colorectal cancer (CRC) is one of the most prevalent and deadly cancers worldwide (Arnold et al., 2017). According to a comprehensive study by the International Agency for Research on Cancer (IARC) published in *Gut* (2020), an estimated 1.9 million new cases and over 930,000 deaths occurred globally in 2020 (Sung et al., 2021). The disease shows significant geographic variation, with the highest incidence in Europe and Australia/New Zealand and the highest mortality in Eastern Europe (Bray et al., 2018). By 2040, the global burden of CRC is projected to rise sharply to 3.2 million new cases (a 63% increase) and 1.6 million deaths (a 73% increase) (Arnold et al., 2020). Over 80% of these new cases are expected to occur in countries with high or very high Human Development Index (HDI) levels (Siegel et al., 2023). While screening programs in high-income nations have helped reduce incidence rates, increasing cases among younger adults and populations in transitional economies remain a growing concern (Vuik et al., 2019; Dekker et al., 2019**)**

WHO Classification of Colorectal Cancer (2021, 5th Edition) – Short & Attractive

Colorectal cancer (CRC) is a biologically diverse disease classified by location, molecular pathways, and histology. Based on anatomy, CRC is divided into right-sided (proximal) tumours arising from the midgut (40–45%) and left-sided (distal) tumours originating from the hindgut (50–60%). Molecularly, CRC develops through three major pathways: chromosomal instability (CIN) (65–70%), microsatellite instability (MSI) (~15%), and the CpG island methylator phenotype (CIMP) (~20%), each contributing uniquely to tumor initiation and progression.

Histologically, adenocarcinoma is the dominant subtype (>90%), followed by mucinous, medullary, and signet ring cell carcinomas, while rare variants include neuroendocrine tumours, serrated CRC, micropapillary carcinoma, GISTs, lymphomas, and sarcomas. This classification highlights the complexity of CRC and guides precise diagnosis, prognosis, and targeted therapy.

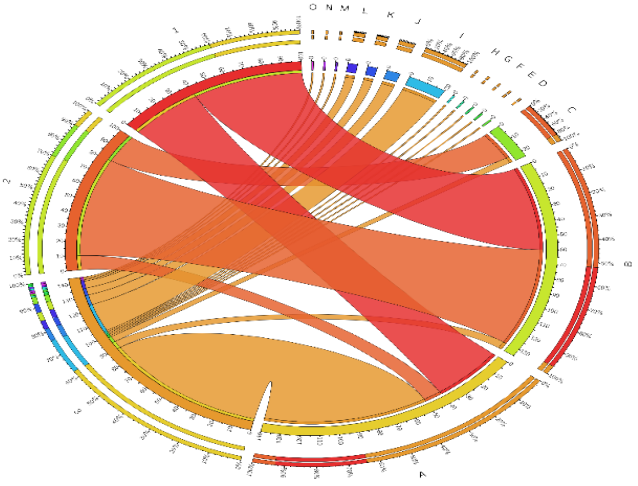

Figure 1: Circular plot chart for WHO Classification of Tumours

Table 1: Colorectal Cancer (Cases) Mortality, 2022.

Colorectal Cancer (Cases) Mortality, 2022.						
0-5000	**5001-10000**	**10001-20000**	**20001-30000**	**30001-50000**	**50001-100000**	**100001-1000000**
Norway	Australia	South Korea	Brazil	Russia	India	China
Singapore	Canada	Poland			USA	
South Africa		Spain			Japan	
		UK				
		Indonesia				

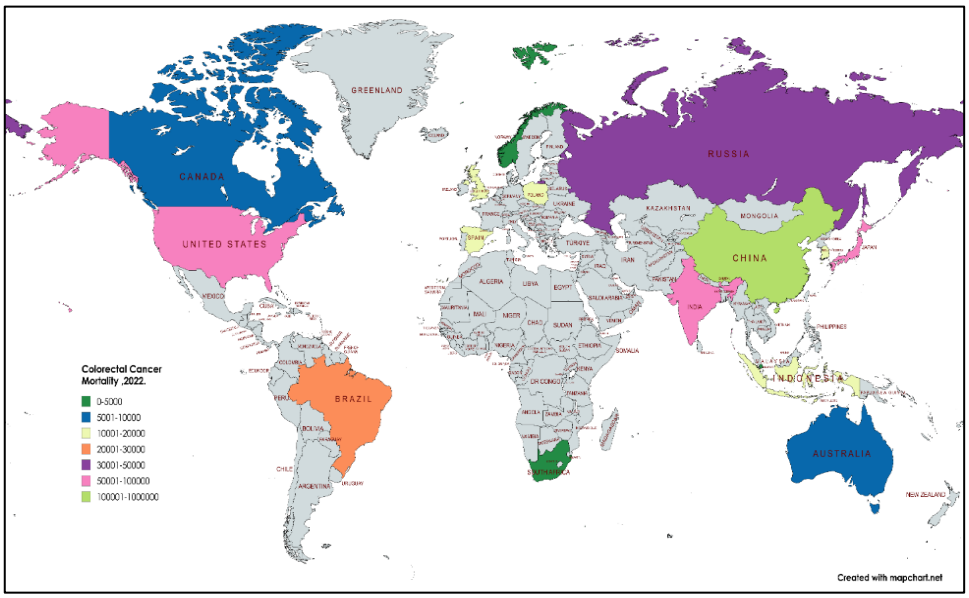

Figure 2: World-wide Scenario on death cases of Colorectal Cancer Population: 0-5000: Norway (1,533), Singapore (2,043), South Africa (4,591). 5001-10000: Australia (8,000), Canada (9,000). 10001-20000: South Korea (11,000), Poland (11,000), Spain (15,000), UK (16,000), Indonesia (19,255). 20001-30000: Brazil (28,884). 30001-50000: Russia (45,309). 50001-100000: India (51,191), USA (52,580), Japan (53,088). 100001-1000000: China (240,010).

The study highlights the critical importance of prevention, particularly through lifestyle modification (reducing obesity, alcohol use, and unhealthy diets) and early detection of precancerous lesions (World Health Organization, 2022). Effective screening and timely removal of polyps have already contributed to declining mortality and over one million survivors worldwide (Siegel et al., 2023). Risk factors include Crohn's disease, colon polyps, advancing age, hereditary predisposition, obesity, and heavy alcohol consumption (Dekker et al., 2019; Keum & Giovannucci, 2019). Common symptoms are changes in bowel habits (diarrhea or constipation), narrow stools, blood in stools, abdominal pain, fatigue, and unintended weight loss (Brenner et al., 2014; Kuipers et al., 2015; Rawla et al., 2019).

Cancer staging helps determine disease progression:

- **Stage 0:** Cancer limited to the innermost intestinal layer
- **Stage I:** Tumor confined to the colon or rectal wall
- **Stage II:** Tumor extends into the muscle layer
- **Stage III:** Spread to regional lymph nodes
- **Stage IV:** Metastasis to distant organs

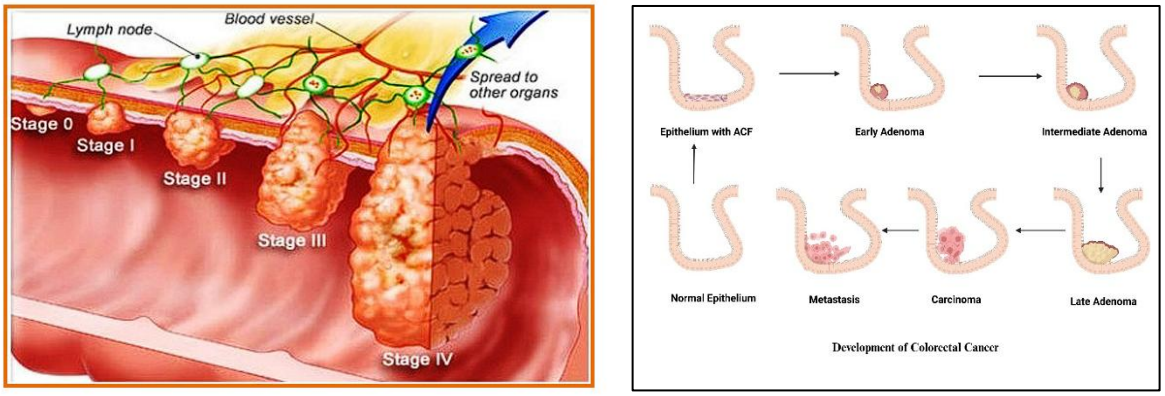

Figure 3: a. Colon with various stages of colorectal cancer b. Development of Cancer

The present study titled *"In Vivo Investigation of the Effect of Intermittent Fasting on Beclin-1 and Bcl-2 Involved in Autophagy and Apoptosis in Colorectal Cancer"* aims to explore this interplay between Beclin-1 (a pro-autophagic marker) and Bcl-2 (an anti-apoptotic regulator), both of which serve as key molecular switches linking these two pathways (Maiuri et al., 2007). Beclin-1 forms part of the autophagy-initiating complex, whereas Bcl-2 binds to Beclin-1, suppressing autophagic flux and promoting cell survival (Pattingre et al., 2005). Therefore, modulation of these proteins can determine whether a cancer cell undergoes survival or death (Kang et al., 2011).

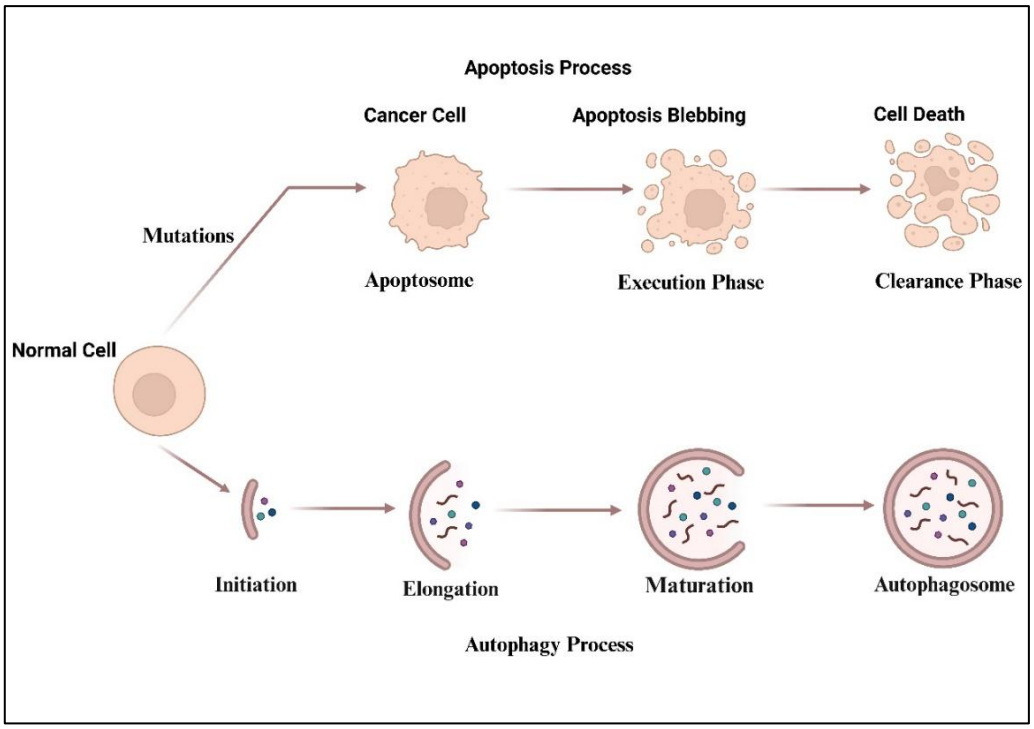

Figure 4: Apoptosis Process

Intermittent fasting (IF) offers a promising non-pharmacological approach to influence these molecular events (de Cabo & Mattson, 2019). Fasting imposes metabolic stress that can reactivate autophagic clearance of damaged cellular components, restore proteostasis, and sensitize tumor cells to apoptosis (Rangan et al., 2019).

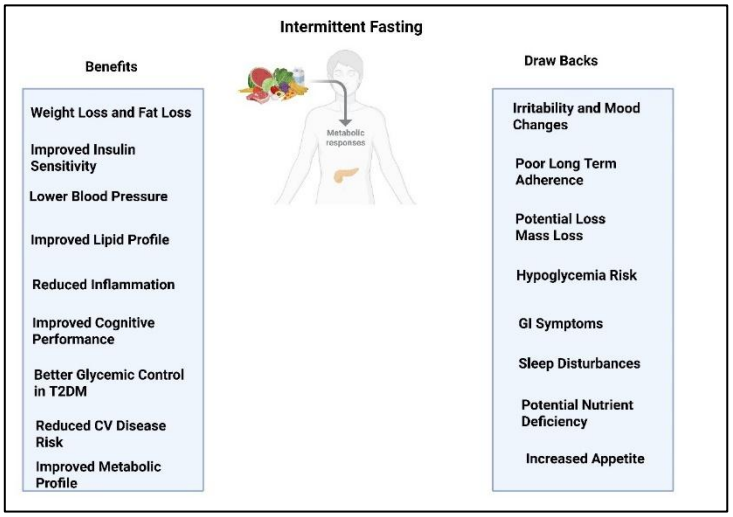

Figure 5: Intermittent Fasting Benefits and Draw Backs

Beclin-1 acts as a key regulator of autophagy by forming multiple protein complexes that either activate or inhibit the process. Its interaction with the Vps34–Vps15 (PI3KC3-I) complex initiates autophagosome formation, while association with UVRAG (PI3KC3-II) promotes autophagosome maturation and endocytic trafficking. Conversely, binding with Rubicon suppresses autophagy by inhibiting maturation. Beclin-1 also interacts with AMBRA1 to enhance autophagy and maintain mitochondrial homeostasis. Its binding to Bcl-2 or Bcl-xL negatively regulates autophagy, whereas ATG14L directs the complex to the phagophore assembly site. Additionally, HMGB1 promotes autophagy by disrupting the inhibitory Beclin-1–Bcl-2 interaction.

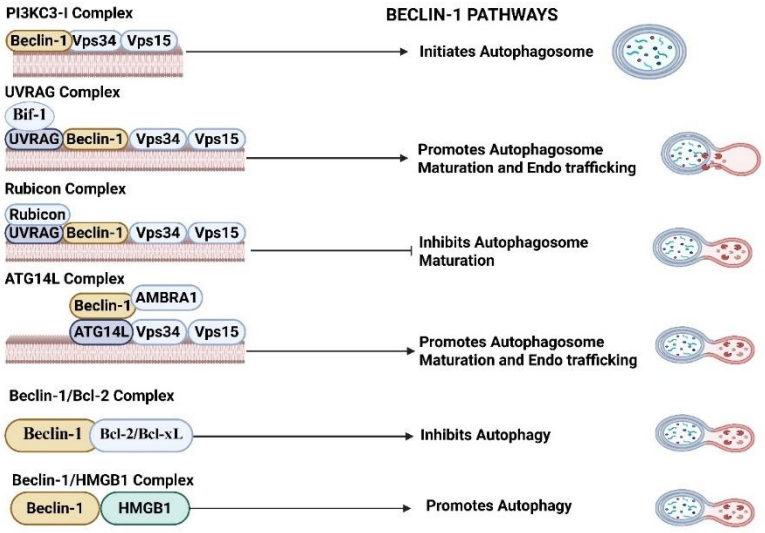

Figure 6: Beclin -1 Pathways

By altering the expression balance between Beclin-1 and Bcl-2, IF may shift cellular homeostasis from survival toward controlled cell death, thereby limiting tumor growth. This mechanistic exploration is crucial to understanding how metabolic interventions like fasting can influence CRC pathophysiology and therapeutic outcomes (Antunes et al., 2020).

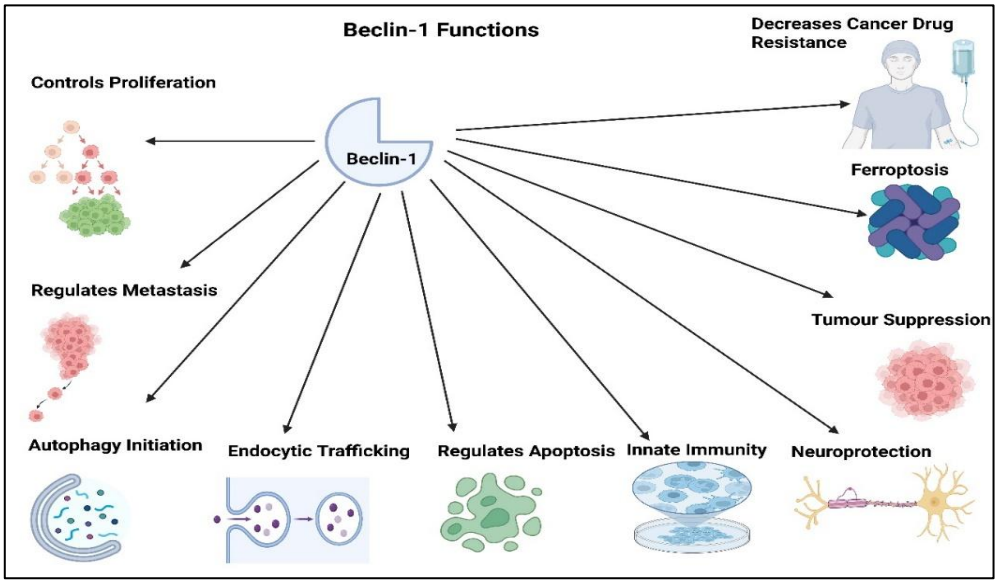

Figure 7: Beclin -1 Functions

MATERIALS AND METHODS

A. Experimental design

Following the successful induction of cancer using a syngeneic rat model, animals will be randomly assigned to eight experimental groups. Each group will consist of **six animals (n = 6)**. The division is structured to evaluate the impact of **intermittent fasting (IF)** at different durations, alongside test and standard treatments. The experimental design is detailed below:

Group Allocation and Description

Table 2: Experimental Grouping for In-Vivo Analysis

Group No.	Group Name	Description
Group I	Normal Control	Healthy rats without cancer induction; standard diet and water ad libitum.
Group II	Disease Control	Cancer-induced rats without any intervention (no fasting or treatment).
Group III	IF – 6 Hours	Cancer-induced rats subjected to 6 hours fasting daily (18-hour feeding window).
Group IV	IF – 12 Hours	Cancer-induced rats subjected to 12 hours fasting daily (12-hour feeding window).
Group V	IF – 18 Hours	Cancer-induced rats subjected to 18 hours fasting daily (6-hour feeding window).
Group VI	IF – 24 Hours (Alternate Day Fasting)	Cancer-induced rats fasted for 24 hours on alternate days (ADF protocol).
Group VII	Standard Drug Treatment	Cancer-induced rats treated with standard anticancer drug (e.g., Doxorubicin).

Note: Each group will consist of **6 animals (n = 6)**.

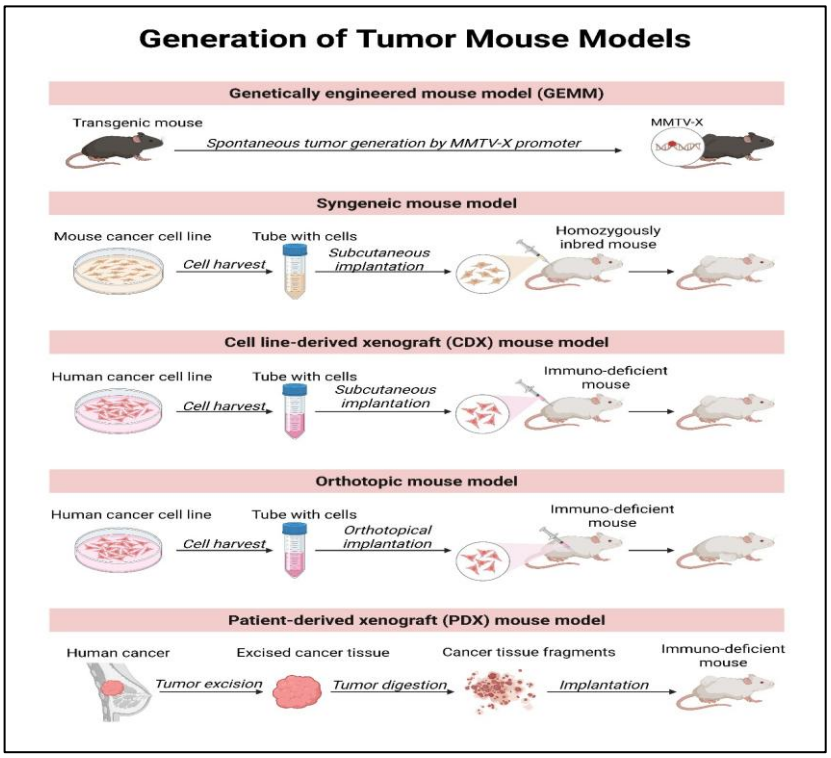

Figure 8: Generation of Tumor Mouse Models

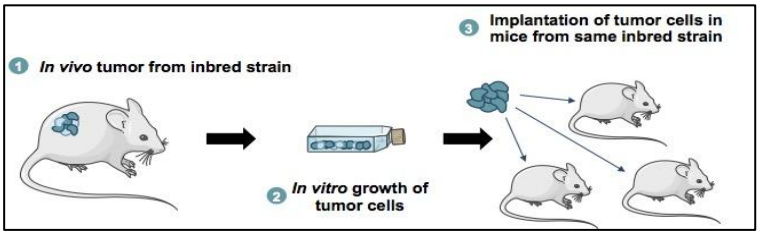

Figure 9: Implantation Mouse model

Assessment of cancer by ACF (Bird, R. P., 1987)

They were sacrificed at eight weeks, and entire colorectums were carefully removed and opened longitudinally from the cecum to the anus. Colorectums were washed with warm PBS to remove feaces and mucus from the surface of mucosa, onto which 10 mL of DNAT-Me (200 µM) was then sprayed. Chronological fluorescence images were taken and stored digitally using a Macro Zoom Microscope (MVX/DP80, Olympus Corp.). Subsequently, the tissues were fixed in 10% formalin for 24 h, and stained with 0.2% methylene blue to observe ACF under a stereomicroscope. The fluorescence intensity of ACF was quantitated using Image J software and normalized to control levels.

1. Histopathological Analysis

a. Haematoxylin and Eosin (H&E) Staining (Sravya et al., 2018)

Tissue sections were fixed, embedded in paraffin, and sectioned onto glass slides. The slides were deparaffinized using three changes of xylene (2 min each) and rehydrated sequentially through graded ethanol (100%, 95%, and 70%) followed by rinsing in running water. Sections were stained with haematoxylin for 3 min and washed under tap water for 5 min to develop a blue coloration. Subsequently, they were counterstained with eosin Y for 2 min to impart a pink hue to cytoplasmic components. The slides were dehydrated through graded ethanol, cleared in xylene, and mounted with coverslips using Permount. The sections were observed under a light microscope to examine histoarchitecture and cellular morphology.

b. Immunohistochemical (IHC) Assessment (Ramos-Vara, 2005; Zhang et al., 2014)

Thin paraffin sections (4 µm) of colon tissue were deparaffinized in xylene and rehydrated through graded alcohol. Endogenous peroxidase activity was blocked with 3% hydrogen peroxide, and nonspecific binding was minimized using 5% BSA in Tris-buffered

saline (TBS) for 1 h. Sections were incubated overnight at 4°C with primary antibodies (anti-PCNA, anti-Ki67, anti-iNOS, and anti-COX-2) diluted 1:500 in TBS containing 5% BSA. After washing, the sections were incubated with HRP-conjugated anti-rabbit secondary antibody (1:2000) for 1 h at room temperature, followed by treatment with 0.02% diaminobenzidine (DAB) containing 0.01% hydrogen peroxide for 5–10 min to visualize antigen–antibody complexes. The slides were counterstained with haematoxylin, dehydrated, mounted, and examined microscopically under a 40× objective.

c. TUNEL Assay (Lebon et al., 2015)

Apoptotic DNA fragmentation was evaluated by the TUNEL assay. Cells were fixed in 4% paraformaldehyde containing 0.12 mM sucrose for 15 min and permeabilized with 0.1% Triton X-100 in 0.1% sodium citrate for 2 min at room temperature. After PBS washing, nonspecific binding was blocked using 10% BSA for 1 h. Coverslips were incubated overnight at 4°C with neuron-specific tubulin antibody (clone Tuj1, 1:1000 dilution), followed by incubation with fluorescein-labeled TUNEL reaction mixture (containing nucleotide mix and terminal deoxynucleotidyl transferase enzyme) for 1 h at 37°C. After washing, cells were mounted using fluorescence-compatible medium and visualized under a fluorescence microscope. TUNEL-positive nuclei indicated apoptotic cells.

2. Biochemical Analysis

a. Western Blotting (Priault et al., 2010)

Protein lysates were prepared by homogenizing 5 mg of tissue in 300 µL of ice-cold lysis buffer, followed by agitation for 2 h at 4°C. The homogenate was centrifuged at 12,000 rpm for 20 min at 4°C, and the supernatant was collected. Equal amounts of protein were denatured with loading buffer, separated by SDS-PAGE (12–16%), and electro transferred to PVDF membranes. Membranes were blocked for 1 h at room temperature with blocking buffer, incubated overnight at 4°C with primary antibodies against NF-κB, TNF-α, IL-6, Bcl-2, Bax, cleaved caspase-3, cleaved caspase-9, and β-actin, followed by HRP-conjugated goat anti-rabbit secondary antibody. Protein bands were visualized using chemiluminescent substrate (ECL Plus) and imaged using a gel documentation system.

b. Enzyme-Linked Immunosorbent Assay (ELISA) (Chen et al., 2017)

Quantification of oxidative stress markers including malondialdehyde (MDA), superoxide dismutase (SOD), catalase (CAT), and glutathione peroxidase (GPx) was performed using standard ELISA kits. In each well of a 96-well plate, capture antibodies (10D7) were coated and blocked with dilution buffer, followed by addition of samples or standards. After incubation and washing, biotinylated detection antibody (AF2666) was added, followed by streptavidin–HRP conjugate. Substrate solution was then added to develop color, and absorbance was measured at 450 nm using a microplate reader. Enzyme activities were calculated from the standard curve.

c. Caspase-3 Activity Assay (Von Ahsen et al., 2000)

Caspase-3 enzymatic activity was determined using the synthetic substrates DEVD-pNA or DEVD-AFC. Briefly, 2 µL of cell or tissue extract was mixed with 200 µL of assay buffer containing 40 µM substrate. For chromogenic assays, absorbance was recorded at 405 nm; for fluorometric assays, emission at 505 nm (excitation 400 nm) was measured over 30 min at room temperature. Increased absorbance or fluorescence indicated enhanced caspase-3 activity.

3. Molecular Biology Analysis

a. Quantitative Real-Time PCR (qRT-PCR) (Heid et al., 1996; Cao & Sethumadhavan, 2022)

Total RNA was isolated from colon tissues using the RNeasy Mini Kit and reverse-transcribed into cDNA. Quantitative PCR was performed using gene-specific TaqMan probes on a StepOne Plus Real-Time PCR System with the following conditions: 50°C for 2 min, 95°C for 10 min, followed by 40 cycles of 95°C for 15 s and 60°C for 1 min. Expression levels were normalized to 18S rRNA, and relative gene expression was calculated using the ΔΔCt method. Standard curves confirmed assay efficiency.

b. Flow Cytometry (Mușina et al., 2021)

Peripheral blood (4 mL) was collected in EDTA tubes and processed within 24 h. Samples were lysed using Bulk Lysis solution, centrifuged, and washed with erythrocyte lysis solution supplemented with 0.5% BSA. Cells were stained with CD3, CD8, and CD45 surface markers and fixed with Fix&Perm reagents A and B. Intracellular markers CK20-FITC and CK7-PE were then applied. After washing, samples were acquired using a FACS Navios flow cytometer, and data were analyzed with Infinicyt software to quantify circulating tumor cells and immune subsets.

c. In Situ Hybridization (ISH) (Chu et al., 2019)

Fixed tissue sections were hybridized with labelled nucleic acid probes complementary to target DNA or RNA sequences. Hybridization was conducted under optimized temperature and salt conditions (15–25°C below the probe Tm). After stringent washing to remove unbound probes, hybridized sequences were visualized via chromogenic or fluorescent detection. This method allowed localization of gene expression within tissue architecture.

d. RNA Sequencing (RNA-seq) (Lee et al., 2024)

High-quality RNA (RIN >7) was extracted from fresh-frozen colorectal tumor and adjacent normal tissues using the RNeasy Mini Kit. Following rRNA depletion

with the Ribo-Zero Gold Kit, cDNA libraries were constructed using the TruSeq RNA Sample Prep Kit. Libraries were sequenced (2 × 100 bp, paired-end) on an Illumina HiSeq 2000 platform. Raw reads were quality-checked, aligned to the reference genome, and analyzed using bioinformatics tools (e.g., DESeq2, edgeR) to identify differentially expressed genes related to apoptosis and autophagy.

4. RESULTS AND DISCUSSION

Assessment of cancer by ACF

The number of crypts per ACF increased significantly to the 12th week in the middle and distal colon (Figure 2B). At the 12th week 46.7% ACF had three or more crypts. ACF morphology consisting of multiple crypts observed to the 12th week may correspond to the promotion step of colon carcinogenesis.

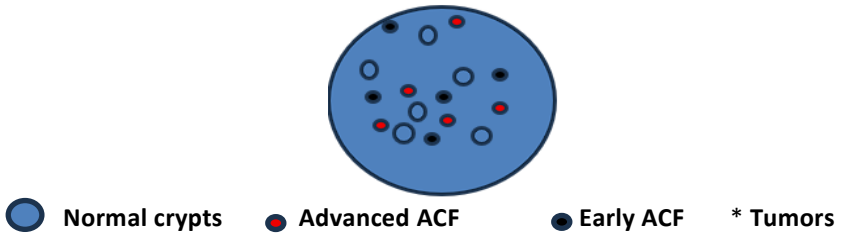

Figure 10: Representative Schematic Showing Normal Crypts, Early ACF, Advanced ACF, and Tumor Formation. The histological progression from normal crypts to early ACF, advanced ACF, and tumours. It visually demonstrates structural changes associated with increasing severity of colonic lesions.

Table 3: Determination of Aberrant Crypt Foci (ACF) Percentage Based on Number of Crypts

Sr. No.	ACF %	No. of Crypts
1	46.7 ±0.22%	5
2	89.7±0.23%	2

Table shows that the percentage of aberrant crypt foci (ACF %) and the number of crypts varied between the two experimental groups. The group with an ACF percentage of 46.7 ± 0.22% exhibited 5 crypts, whereas the group with a higher ACF percentage of 89.7 ± 0.23% exhibited only 2 crypts. From the table, it can be observed that as the ACF percentage increases, the number of crypts decreases, indicating an inverse relationship between these two parameters. This suggests that higher aberrant crypt foci percentage is associated with reduced crypt count in the studied samples.

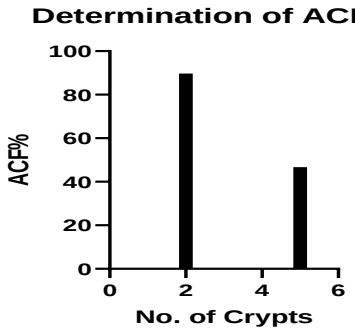

Graph 1: Graphical Representation of ACF Percentage in Relation to Number of Crypts

Relationship between crypt number and ACF percentage. As the number of crypts per focus decreases, ACF% increases, indicating a progression toward advanced preneoplastic changes.

Histopathological Assessment of Apoptotic and Autophagic Markers

Table 4: Histopathological Evaluation of Beclin-1 Expression

Sr. No.	Groups	Histopathological Image	Observations
1	IF – 6 Hours	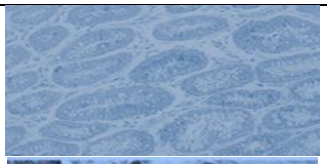	Slight improvement in tissue structure; mild reduction in kidney damage.
2	IF – 12 Hours	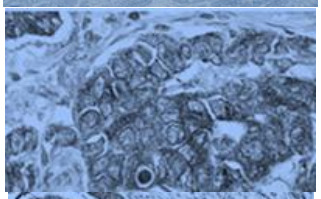	Moderate tissue recovery; decreased inflammation and cellular disorganization.
3	IF – 18 Hours	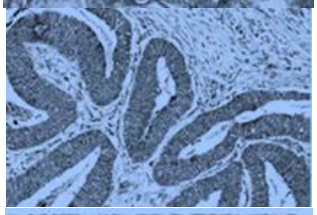	Noticeable restoration of normal glomerular and tubular structure; less degeneration.
4	IF – 24 Hours (Alternate Day Fasting)	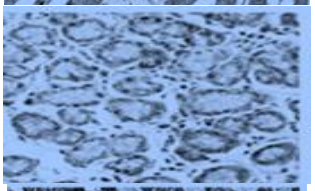	Strong protection; clear renal histoarchitecture with minimal pathological alterations.
5	Standard Drug Treatment	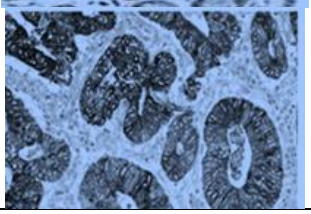	Effective recovery; renal cells appear close to normal indicating strong therapeutic effect.

Table 5: Histopathological Evaluation of Bcl-2 Protein Expression

S.No.	Groups	Histopathological Image	Observations
1	IF – 6 Hours	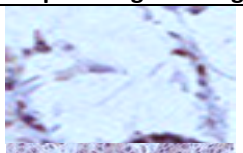	Mild improvement observed. Slight reduction in tubular degeneration and glomerular swelling.
2	IF – 12 Hours	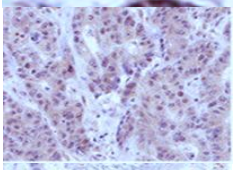	Moderate renal recovery. Noticeable reduction in inflammation and structural disorganization.
3	IF – 18 Hours	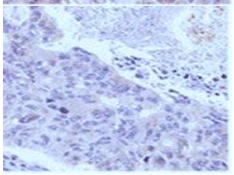	Significant preservation of kidney architecture. Reduced necrosis and inflammation.

4	IF – 24 Hours (Alternate Day Fasting)	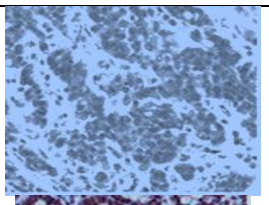	Remarkable renal protection. Tubules and glomeruli appear near-normal with minimal pathological signs.
5	Standard Drug Treatment	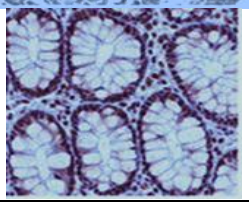	Excellent recovery. Normal renal histology restored, comparable to healthy kidney tissue.

Table 6: Histopathological study of Colon

S.No.	Groups	Histopathological Image	Observations
1	IF – 6 Hours		Slight tubular damage; mild inflammation; limited structural recovery.
2	IF – 12 Hours		Moderate reduction in tubular necrosis and interstitial inflammation; improved glomerular appearance.
3	IF – 18 Hours	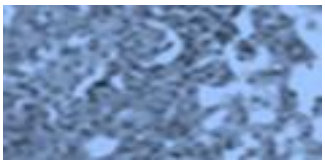	Significant renal protection; well-preserved tubules and glomeruli with reduced cellular damage.
4	IF – 24 Hours (Alternate Day Fasting)		Near-normal kidney structure; minimal pathological lesions; strong anti-inflammatory effect observed.
5	Standard Drug Treatment	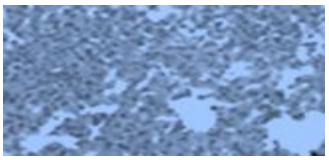	Renal architecture almost restored; minimal degeneration; comparable to normal kidney tissue.

Table 7: Histopathological study of the Rectum

S.No.	Groups	Histopathological Image	Observation
1	IF – 6 Hours	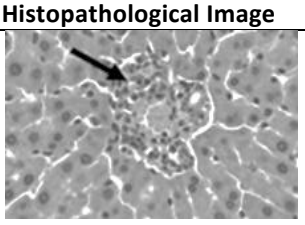	Mild tubular degeneration and slight inflammation. Early signs of renal protection.

2	IF – 12 Hours	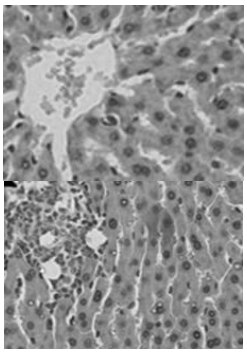	Moderate reduction in necrosis; improved glomerular and tubular integrity.
3	IF – 18 Hours		Clear structural recovery; reduced inflammatory infiltrates and tubular damage.
4	IF – 24 Hours (Alternate Day Fasting)	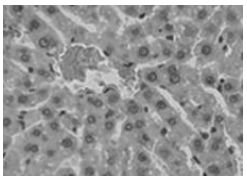	Prominent tissue protection; near-normal glomeruli and tubules; minimal pathology
5	Standard Drug Treatment	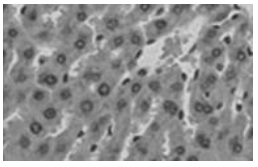	Almost complete renal restoration; minimal cellular damage; comparable to healthy control.

Immunohistochemical Assessment of Apoptotic and Autophagic Markers

Table 8: Immunohistochemical expression of Beclin-1 and Bcl-2 in experimental groups

Description	Beclin-1 expression	Bcl-2 Expression
Normal	0	0
Disease Control	1	1
IF – 6 Hours	1	1
IF – 12 Hours	2	2
IF – 18 Hours	2	2
IF – 24 Hours	3	3
Standard Drug Treatment	1	1

Table shows the effect of intermittent fasting and standard treatment on Beclin-1 and Bcl-2 expression in different experimental groups. The normal control group showed no expression (0) for both Beclin-1 and Bcl-2, while the disease control group exhibited a mild expression level of 1 for both markers. Treatment with intermittent fasting for 6 and 12 hours showed expression scores of (1,1) and (2,2) respectively for Beclin-1 and Bcl-2, indicating a gradual increase in expression with longer fasting duration. Further increase was observed in the 18-hour fasting group with (2,2) and the 24-hour (alternate day fasting) group showing the highest expression score of (3,3) for both markers. The standard drug treatment group demonstrated a mild expression level of (1,1). From the table, it can be observed that intermittent fasting duration is directly associated with increased Beclin-1 and Bcl-2 expression, with the 24-hour fasting group showing the most significant expression compared to other treated groups.

Table 9. Distribution of Beclin-1 and Bcl-2 Expression Intensity by Frequency and Percentage

Intensity of Beclin 1 and Bcl-2	Frequency	%
0	6	14
1	18	42
2	12	28
3	6	14

Table shows the distribution of Beclin-1 and Bcl-2 expression intensity along with their frequency and percentage in the studied samples. An intensity score of 0 was observed in 6 samples, accounting for 14% of the total. The majority of samples (18, 42%) exhibited an intensity score of 1. Moderate expression with a score of 2 was found in 12 samples (28%), while the highest expression score of 3 was recorded in 6 samples (14%). From the table, it can be observed that low to moderate expression (scores 1 and 2) was more prevalent compared to no expression (score 0) or high expression (score 3), indicating that most experimental subjects exhibited mild to moderate Beclin-1 and Bcl-2 expression.

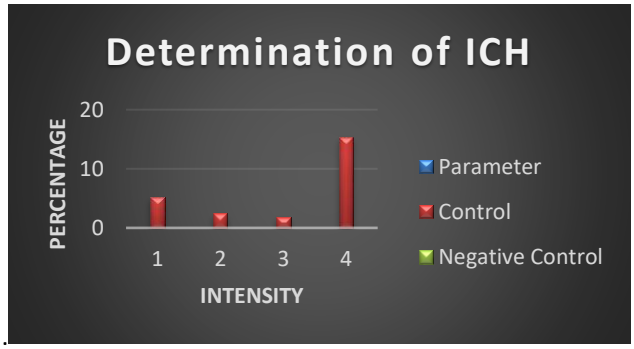

Graph 3. Determination of intensity of Beclin-1 and Bcl-2 expression

Graph 3 shown the intensity distribution of Beclin-1 and Bcl-2 expression. Most samples exhibited mild (42%) or moderate (28%) staining, while high (14%) and absent (14%) expression levels were less common. This suggests that Beclin-1 and Bcl-2 are predominantly expressed at low to moderate levels in the studied samples.

TUNEL Assay (Terminal deoxynucleotidyl transferase dUTP Nick End Labelling) for autophagy & apoptosis index

Table 10: Apoptosis and autophagy index in experimental groups

Groups	Apoptosis Index	Autophagy Index
Normal	21.5±1.12	20.5±1.22
Disease Control	20.5±1.02	21.2±1.52
IF – 6 Hours	19.5±0.92	21.4±1.02
IF – 12 Hours	21.4±1.14	18.5±1.11
IF – 18 Hours	22.5±1.32	19.5±1.08
IF – 24 Hours (Alternate Day Fasting)	18.5±1.02	21.6±1.17
Standard Drug Treatment	20.5±1.42	22.5±1.18

Table 10 shows the apoptosis index and autophagy index values for different experimental groups. The normal control group (I) recorded mean values of 21.5 ± 1.12 for apoptosis and 20.5 ± 1.22 for autophagy. The disease control group (II) exhibited slightly lower apoptosis (20.5 ± 1.02) and slightly higher autophagy (21.2 ± 1.52) compared to normal control. Groups III and IV displayed apoptosis indices of 19.5 ± 0.92 and 21.4 ± 1.14, with corresponding autophagy values of 21.4 ± 1.02 and 18.5 ± 1.11, indicating varied effects based on treatment type. Group V showed the highest apoptosis index (22.5 ± 1.32) with moderate autophagy (19.5 ± 1.08). Group VI demonstrated the lowest apoptosis index (18.5 ± 1.02) but relatively high autophagy (21.6 ± 1.17), while group VII exhibited balanced values with apoptosis at 20.5 ± 1.42 and the highest autophagy index (22.5 ± 1.18). From the table, it can be observed that treatments influence apoptosis and autophagy differently, with group V showing maximum apoptosis and group VII showing maximum autophagy compared to other treated groups.

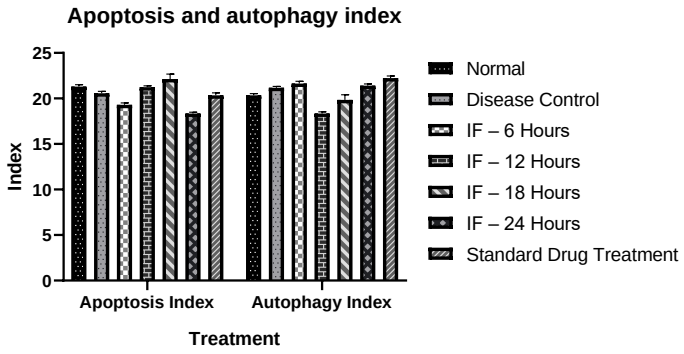

Graph 4: Determination of autophagy and apoptosis index across in groups

Graph 4 compares mean apoptosis and autophagy indices among different experimental groups. Group V (IF – 18h) showed the highest apoptosis index, while Group VII (standard drug) demonstrated the highest autophagy index. Overall, both indices remained relatively stable across groups, with slight variations indicating time-dependent responses to intermittent fasting and treatment interventions.

Biochemical Analysis

Determination of NF-KB and inflammatory cytokine expression by Western Blotting

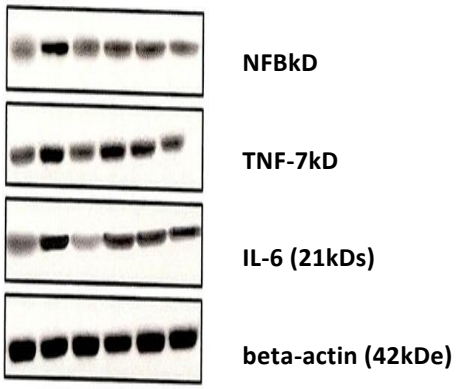

Figure 11: Immunoblot analysis of NF-KB, TNF-a, and IL-6 in the colon tissue of control and experimental rats. Lane 1: control, lane 2: 6 hours IF; lane 3: 12 hours IF; lane 4: 18 hours IF; lane 5: 24 hours IF; lane 6: 5 FU.

Table 11: Quantification of NF-κB, TNF-α, and IL-6 Expression in Colon Tissue (Normalized to β-Actin)

Group	NF-κB	TNF-α	IL-6	β-actin (42 kDa)
I – Control	0.45±0.01	0.40±0.01	0.34±0.01	1.00
II – Negative Control	1.35±0.02	1.30±0.02	1.24±0.02	1.00
III – IF 6h	1.05±0.01	1.00±0.00	0.99±0.01	1.00
IV – IF 12h	0.95±0.02	0.90±0.02	0.85±0.02	1.00
V – IF 18h	0.84±0.03	0.80±0.02*	0.75±0.01	1.00
VI – IF 24h	0.75±0.02*	0.70±0.01*	0.65±0.02*	1.00
VII – Standard Drug	0.65±0.01	0.60±0.02	0.55±0.03	1.00

Table shows the effect of intermittent fasting and standard drug treatment on NF-κB, TNF-α, and IL-6 protein expression in different experimental groups, with β-actin (42 kDa) used as the loading control. The control group (I) displayed the lowest expression levels of NF-κB (0.45 ± 0.01), TNF-α (0.40 ± 0.01), and IL-6 (0.34 ± 0.01). In contrast, the negative control group showed markedly elevated expression levels of NF-κB (1.35 ± 0.02), TNF-α (1.30 ± 0.02), and IL-6 (1.24 ± 0.02), indicating significant inflammatory activation. Treatment with intermittent fasting for 6, 12, 18, and 24 hours (Groups III–VI) resulted in a progressive reduction in the expression of these inflammatory markers, with the lowest levels recorded in the 24-hour fasting group (NF-κB: 0.75 ± 0.02, TNF-α: 0.70 ± 0.01, IL-6: 0.65 ± 0.02). The standard drug treatment group (VII) demonstrated the most pronounced suppression of inflammatory proteins, with NF-κB at 0.65 ± 0.01, TNF-α at 0.60 ± 0.02, and IL-6 at 0.55 ± 0.03. From the table, it can be observed that both intermittent fasting and standard drug treatment markedly reduced pro-inflammatory protein expression compared to the negative control, with the standard drug and 24-hour fasting groups showing the greatest effect.

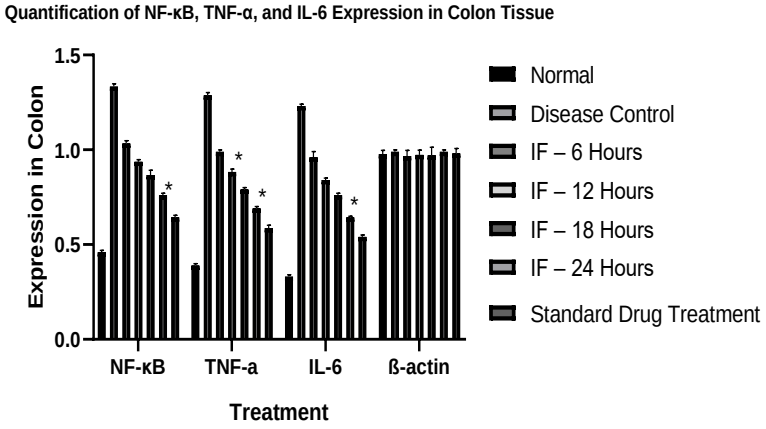

Graph 5. Determination of inflammatory biomarkers (NF-κB, TNF-α, IL-6) in colon tissue of experimental groups

Graph shown the relative expression of inflammatory biomarkers normalized to β-actin. The DMH-treated group showed markedly increased levels of NF-κB, TNF-α, and IL-6. Intermittent fasting resulted in a gradual, time-dependent decrease in these markers, with the most significant reduction observed in the 24-hour IF and standard treatment groups. These findings suggest both intermittent fasting and drug therapy effectively downregulate pro-inflammatory cytokines in colon tissue.

Immunoblot analysis of apoptosis-related proteins in the colon tissue of control and experimental rats.

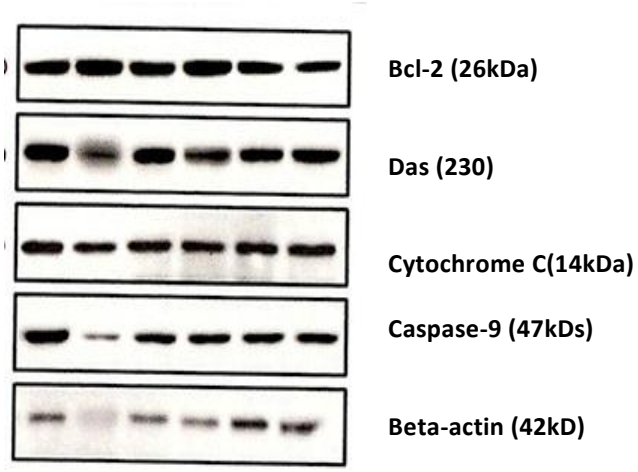

Figure 12: Immunoblot analysis of apoptosis-related proteins in the colon tissue of control and experimental rats. Lane 1: control, lane 2: 6 hours IF; lane 3: 12 hours IF; lane 4: 18 hours IF; lane 5: 24 hours IF; lane 6: 5 FU.

Table 12: Analysis of Apoptotic and Autophagy-Related Proteins (Western Blot) in experimental groups

Group	Bcl-2 (26 kDa)	Bax (23 kDa)	Cytochrome C (14 kDa)	Caspase-9 (47 kDa)	β-actin (42 kDa)
I – Control	1.25	0.55	0.50	0.60	1.00
II – Negative Control	0.46	1.35	1.20	1.25	1.00
III – IF 6h	0.60	1.30	1.15	1.20	1.00
IV – IF 12h	0.86	1.25	1.10	1.10	1.00
V – IF 18h	0.90	1.0	1.02	1.00	1.00
VI – IF 24h	1.10	0.70	0.75	0.89	1.00
VII – Standard	1.21	0.54	0.45	0.65	1.00

Table shows the effect of intermittent fasting and standard treatment on the expression of apoptosis-related proteins Bcl-2 (26 kDa), Bax (23 kDa), Cytochrome C (14 kDa), and Caspase-9 (47 kDa), with β-actin (42 kDa) as the loading control. In the control group (I), a high Bcl-2 value (1.25) with low Bax (0.55), Cytochrome C (0.50), and Caspase-9 (0.60) was observed, indicating basal anti-apoptotic status. The negative control group (II) exhibited a marked decrease in Bcl-2 (0.46) and a notable increase in Bax (1.35), Cytochrome C (1.20), and Caspase-9 (1.25), reflecting enhanced pro-apoptotic activity. Treatment with intermittent fasting for 6, 12, and 18 hours (Groups III–V) gradually increased Bcl-2 expression (0.60, 0.86, 0.90) while decreasing pro-apoptotic markers, with the 18-hour fasting group showing a more balanced Bax/Bcl-2 ratio. The 24-hour fasting group (VI) demonstrated a marked rise in Bcl-2 (1.10) with a notable reduction in Bax (0.70), Cytochrome C (0.75), and Caspase-9 (0.89), suggesting strong anti-apoptotic protection. The standard drug treatment group (VII) showed the highest Bcl-2 (1.21) and lowest pro-apoptotic protein levels (Bax: 0.54, Cytochrome C: 0.45, Caspase-9: 0.65) among all groups. From the table, it can be observed that intermittent fasting, particularly for 24 hours, and standard treatment significantly shifted the balance toward anti-apoptotic signaling compared to the negative control.

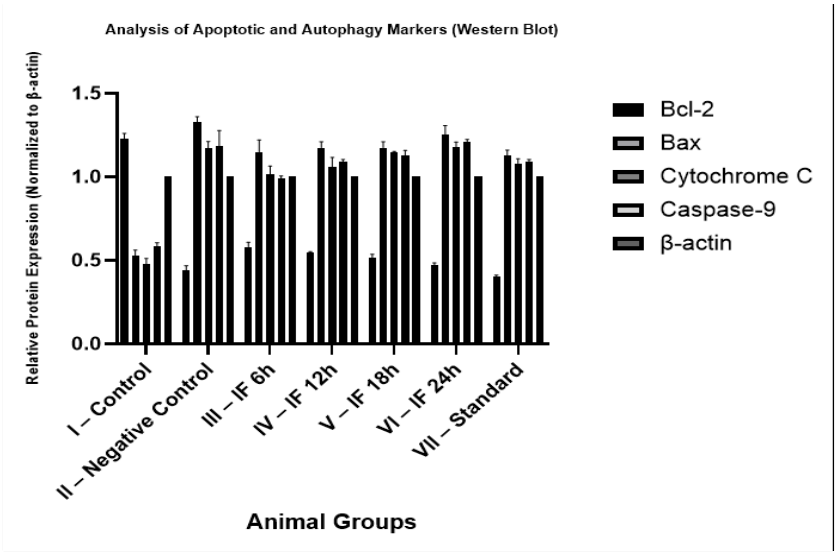

Graph 6: Analysis of Apoptotic and Autophagy Markers (Western Blot)

Graph shown the relative expression of Bcl-2, Bax, Cytochrome C, and Caspase-9 across different treatment groups. The disease group showed elevated pro-apoptotic proteins (Bax, Cytochrome C, Caspase-9) and reduced Bcl-2, indicating apoptosis induction. Intermittent fasting progressively restored Bcl-2 and reduced pro-apoptotic markers, with the 24-hour IF and standard drug groups showing the most normalized profiles, suggesting protective modulation of apoptotic pathways.

ELISA (Enzyme-Linked Immunosorbent Assay)

Table 13: Effect of Embinin in intermittent fasting on oxidative stress in colon cancer

Group	SOD	CAT	GSH	GPx
I – Control	4.14±0.07	4.12±0.07	12.49±0.21c	15.43±0.21c
II – Negative Control	2.14±0.05a	2.94±0.05a	9.74±0.11a	10.93±0.29a
III – IF 6h	2.67±0.08b	2.99±0.06b	9.92±0.40c	11.25±0.31c
IV – IF 12h	3.18±0.07b	3.07±0.07b	11.92±0.41c	12.65±0.20c
V – IF 18h	4.12±0.06b	4.10±0.06b	10.32±0.45b	13.26±0.14b
VI – IF 24h	4.01±0.06b	4.01±0.05b	11.45±0.36c	14.36±0.28c
VII – Standard	4.14±0.07	4.12±0.07	12.49±0.21c	15.43±0.21c

Table shows the effect of intermittent fasting and standard treatment on antioxidant enzyme activities, including superoxide dismutase (SOD), catalase (CAT), reduced glutathione (GSH), and glutathione peroxidase (GPx) in different experimental groups. The control group (I) exhibited the highest baseline antioxidant status with SOD at 4.14 ± 0.07, CAT at 4.12 ± 0.07, GSH at 12.49 ± 0.21, and GPx at 15.43 ± 0.21. The negative control group (II) showed a significant reduction in all antioxidant markers (SOD: 2.14 ± 0.05, CAT: 2.94 ± 0.05, GSH: 9.74 ± 0.11, GPx: 10.93 ± 0.29), indicating oxidative stress. Intermittent fasting for 6 and 12 hours (Groups III and IV) resulted in moderate improvements in antioxidant enzyme levels compared to the negative control, with notable increases in GSH and GPx at 12 hours. The 18-hour fasting group (V) demonstrated SOD and CAT values almost equivalent to the control group, along with improved GPx (13.26 ± 0.14), while the 24-hour fasting group (VI) showed sustained high antioxidant levels across all parameters. The standard treatment group (VII) matched the control group values, showing maximum antioxidant protection. From the table, it can be observed that intermittent fasting, especially for 18 and 24 hours, markedly restored antioxidant Defense systems closer to normal control levels, similar to standard drug treatment.

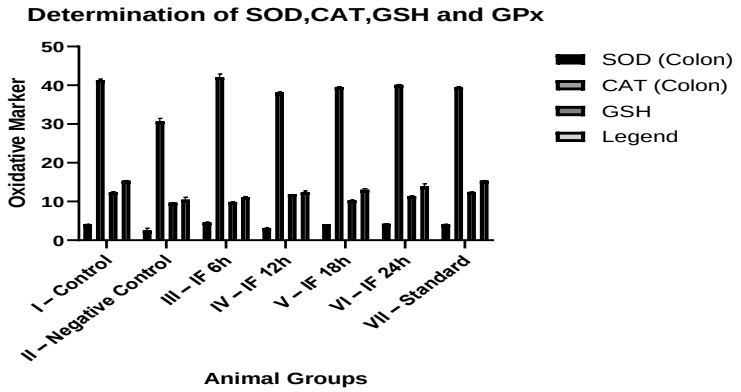

Graph 7. Determination of SOD, CAT, GSH, and GPx levels in experimental groups

Graph shown the antioxidant enzyme activities in colon tissue. The negative control group showed significant depletion of SOD, CAT, GSH, and GPx levels, indicating oxidative stress. In contrast, intermittent fasting—especially for 18 and 24 hours—and the standard treatment group restored these antioxidant levels close to normal, highlighting their protective role against oxidative damage.

Determination of Caspase-3 activity

Figure 13: Analysis of caspase-3 in the colon tissue of control and experimental rats.

Table 14: Analysis of caspase-3 expression in colon tissue (normalized to β-actin) of experimental rat

Group	Caspase-3(47 kDa)	β-actin (42 kDa)
I – Control	0.36	1.00
II – Negative Control	0.19	1.00
III – IF 6h	0.23	1.00
IV – IF 12h	0.26	1.00
V – IF 18h	0.30	1.00
VI – IF 24h	0.32	1.00
VII – Standard	0.35	1.00

Table shows the effect of intermittent fasting and standard treatment on Caspase-3 (47 kDa) expression, with β-actin (42 kDa) used as the loading control. The control group (I) exhibited a Caspase-3 level of 0.36, representing normal baseline apoptotic activity. The negative control group (II) showed a marked reduction in Caspase-3 expression (0.19), indicating suppression of apoptosis under disease conditions. Intermittent fasting for 6, 12, and 18 hours (Groups III–V) resulted in a gradual increase in Caspase-3 levels (0.23, 0.26, and 0.30, respectively) compared to the negative control. The 24-hour fasting group (VI) further increased Caspase-3 expression to 0.32, approaching the control value. The standard drug treatment group (VII) exhibited a Caspase-3 level of 0.35, closely matching the normal control. From the table, it can be observed that intermittent fasting, particularly for 24 hours, and standard treatment effectively restored Caspase-3 expression towards normal levels, suggesting improved apoptotic regulation compared to the negative control.

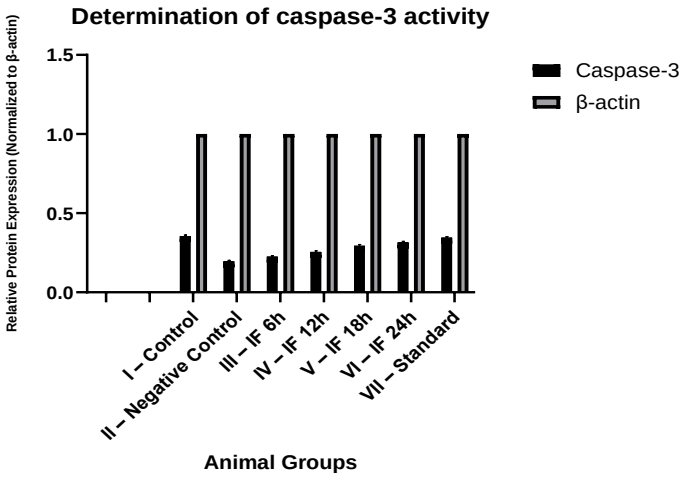

Graph 8: Determination of Caspase-3 Activity in Colon Tissue (Normalized to β-Actin)

Graph shown Caspase-3 protein expression across different experimental groups. The negative control group exhibited reduced Caspase-3 levels, indicating diminished apoptotic activity. Intermittent fasting (IF), especially at 24 hours, progressively enhanced Caspase-3 expression, with the standard drug group showing expression levels similar to the control.

Biomolecular (molecular biology) analysis

Table 15: Gene-Specific Primer Sequences Used for RT-PCR Analysis

Gene	Forward Primer (5′–3′)	Reverse Primer (5′–3′)
β-Catenin	ACTGGCAGCAGCAATCTTAC	GAGGTGTCCACATCTTCTTC
TNF-α	CTTCTGTCTACTGAACTTCG	AAGATGATCTGAGTGTGAGG
NF-κB	GCTTACGGTGGGATTGCATT	TTATGGTGCCATGGGTGATG
iNOS	TAAAGGGACAGCGTCAGCGA	TGGGGGAACACAGTAATGGC
Bax	GGCGAATTGGAGATGAACTG	CCCCAGTTGAAGTTGCCAT
VEGF-α	TATATCTTCAAGCCGTCCTGTG	TCTCCTATGTGCTGGCTTTG
β-actin	TGT TTG AGA CCT TCA ACA CC	TAG GAG CCA GGG CAG TAA TC

These primers were used for RT-PCR to evaluate gene expression profiles in colon tissues subjected to intermittent fasting and standard treatment interventions.

Table 16: Effect of intermittent fasting on m-RNA expression of inflammatory, apoptotic, and angiogenic genes in experimental groups

Group	TNF-α	β-Catenin	NF-κB	iNOS	VEGF-α	BAX
I – Control	1.1±0.51	1.2±0.51	1.3±0.51	1.0±0.51	1.2±0.51	1.5±0.51
II – Negative Control	3.8 ±0.51	2.4 ±0.51	2.7 ±0.51	2.0 ±0.51	2.3 ±0.51	0.8 ±0.51
III – IF 6h	3.6±0.51	2.3±0.51	2.5±0.51	1.9±0.51	2.1±0.51	0.78±0.51
IV – IF 12h	2.6±0.51	2.1±0.51	2.0±0.51	1.7±0.51	1.9±0.51	1.2±0.51
V – IF 18h	2.0±0.51	1.7±0.51	1.8±0.51	1.5±0.51	1.8±0.51	1.0±0.51
VI – IF 24h	1.5±0.51	1.5±0.51	1.7±0.51	1.4±0.51	1.6±0.51	1.4±0.51
VII – Standard	1.2±0.51	1.3±0.51	1.6±0.51	1.2±0.51	1.4±0.51	1.6±0.51

Table shows the effect of intermittent fasting and standard treatment on inflammatory and apoptotic markers, including TNF-α, β-Catenin, NF-κB, iNOS, VEGF-α, and BAX in different experimental groups. The control group (I) exhibited baseline values for all markers, with TNF-α at 1.1 ± 0.51, β-Catenin at 1.2 ± 0.51, NF-κB at 1.3 ± 0.51, iNOS at 1.0 ± 0.51, VEGF-α at 1.2 ± 0.51, and BAX at 1.5 ± 0.51. The negative control group (II) showed marked elevation in pro-inflammatory markers (TNF-α: 3.8 ± 0.51, β-Catenin: 2.4 ± 0.51, NF-κB: 2.7 ± 0.51, iNOS: 2.0 ± 0.51, VEGF-α: 2.3 ± 0.51) along with a reduction in pro-apoptotic BAX (0.8 ± 0.51), indicating a shift toward tumor-promoting conditions. Intermittent fasting for 6 and 12 hours (Groups III and IV) reduced inflammatory marker levels compared to the negative control, with further reductions observed in the 18-hour fasting group (V). The 24-hour fasting group (VI) showed near-normal values, particularly for TNF-α (1.5 ± 0.51), NF-κB (1.7 ± 0.51), and BAX (1.4 ± 0.51), suggesting restored apoptotic balance. The standard treatment group (VII) demonstrated values closest to the control, with the highest BAX level (1.6 ± 0.51) and the lowest inflammatory marker expression. From the table, it can be observed that both intermittent fasting and standard treatment effectively attenuate inflammatory responses and restore apoptotic signaling, with the 24-hour fasting and standard drug groups showing the most prominent improvements compared to the negative control.

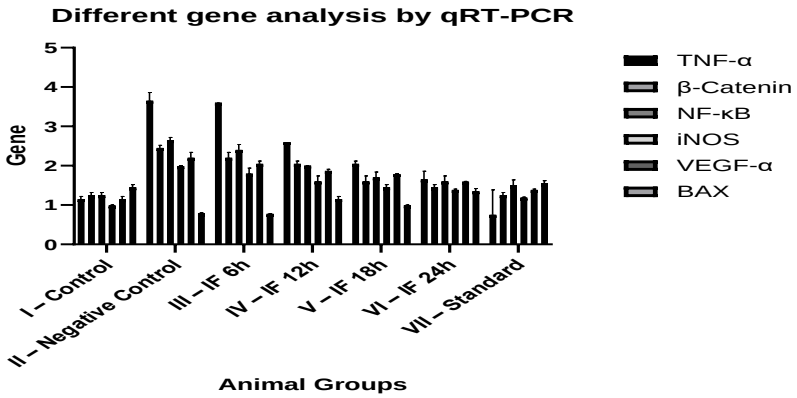

Graph 9: Different Gene Analysis by qRT-PCR

The bar graph represents the expression levels of different genes (TNF-α, β-Catenin, NF-κB, iNOS, VEGF-α, and BAX) across various experimental animal groups as measured by qRT-PCR. In the control group (Group I), baseline levels of all genes are relatively low. The negative control group (Group II – DMH induced) shows a marked increase in pro-inflammatory and oncogenic genes such as TNF-α, β-Catenin, NF-κB, iNOS, and VEGF-α, along with a notable decrease in the pro-apoptotic marker BAX, indicating tumor-promoting conditions. Treatment groups with intermittent fasting (Groups III–VI) show a progressive reduction in inflammatory and cancer-associated gene expression, with the most pronounced downregulation observed in the IF 24 h group (Group VI). This group also displays a relative increase in BAX expression, suggesting a shift toward apoptosis. The standard drug treatment group (Group VII) demonstrates similar effects to IF 24 h, with substantial suppression of TNF-α, β-Catenin, NF-

κB, iNOS, and VEGF-α, while maintaining elevated BAX levels, highlighting both anti-inflammatory and pro-apoptotic potential.

From the pattern, it can be inferred that intermittent fasting, especially for longer durations (24 h), and standard drug administration both effectively counteract tumor-related gene expression changes induced by DMH.

Table 17: Flow Cytometry Analysis in Colon Cancer Rat Model

Group	Early Apoptosis (%)	Late Apoptosis (%)	Necrosis (%)	CD4+ T cells (%)	CD8+ T cells (%)	Ki-67+ Proliferation (%)
Control	5.1±0.3	5.1±0.1	2.5±0.3	15.2±0.3	11.9±0.2	6.0±0.2
Negative Control	2.1±0.4	1.0±0.3	3.4±0.2	9.0±0.2	7.5±0.2	12.2±0.2
IF – 6 h	3.2±0.2	1.3±0.3	3.1±0.1	9.6±0.2	7.6±0.3	11.6±0.2
IF – 12 h	3.8±0.1	1.6±0.2	2.5±0.2	10.2±0.2	8.0±0.2	10.6±0.1
IF – 18 h	4.1±0.2	1.8±0.1	2.3±0.2	12.5±0.2	8.8±0.2	9.5±0.1
IF – 24 h	4.6±0.2	2.2±0.2	2.1±0.3	13.1±0.3	10.2±0.1	8.2±0.2
Standard	4.9±0.3	2.3±0.3	1.8±0.3	14.2±0.3	12.1±0.1	6.7±0.2

Table shows the effect of intermittent fasting and standard treatment on apoptosis stages, necrosis, T-cell populations, and cell proliferation in different experimental groups. The control group exhibited early apoptosis of 5.1 ± 0.3% and late apoptosis of 5.1 ± 0.1%, with a low necrosis rate (2.5 ± 0.3%). $CD4^+$ and $CD8^+$ T cells were at 15.2 ± 0.3% and 11.9 ± 0.2%, respectively, and Ki-67^+ proliferation was 6.0 ± 0.2%. The negative control group showed reduced early (2.1 ± 0.4%) and late apoptosis (1.0 ± 0.3%), increased necrosis (3.4 ± 0.2%), decreased $CD4^+$ (9.0 ± 0.2%) and $CD8^+$ (7.5 ± 0.2%) T cells, and a marked increase in proliferation (12.2 ± 0.2%), indicating tumor-promoting conditions. Intermittent fasting for 6 and 12 hours (Groups III and IV) moderately improved apoptotic indices and T-cell percentages, with reduced proliferation compared to the negative control. The 18-hour fasting group (V) showed further increases in early apoptosis (4.1 ± 0.2%) and $CD4^+$ T cells (12.5 ± 0.2%). The 24-hour fasting group (VI) recorded early apoptosis of 4.6 ± 0.2%, late apoptosis of 2.2 ± 0.2%, and improved $CD4^+$ (13.1 ± 0.3%) and $CD8^+$ (10.2 ± 0.1%) T cells, along with reduced proliferation (8.2 ± 0.2%). The standard drug treatment group (VII) demonstrated values close to the control, with early apoptosis at 4.9 ± 0.3%, late apoptosis at 2.3 ± 0.3%, high $CD4^+$ (14.2 ± 0.3%) and $CD8^+$ (12.1 ± 0.1%) T-cell percentages, and low proliferation (6.7 ± 0.2%). From the table, it can be observed that intermittent fasting, especially for 24 hours, and standard drug treatment effectively restored apoptosis, enhanced immune response, and reduced tumor cell proliferation compared to the negative control.

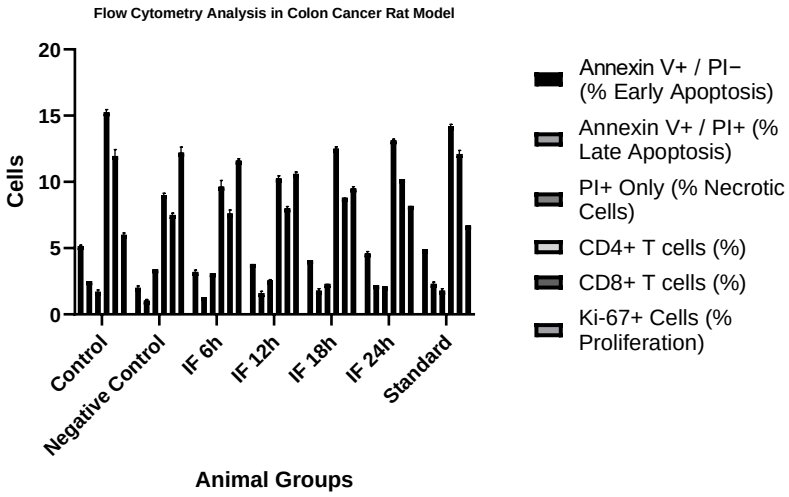

Graph 10: Flow cytometry analysis in colon cancer rat model

Flow cytometry analysis revealed variations in early apoptosis (Annexin V+/PI$^-$), late apoptosis (Annexin V$^+$/PI$^+$), necrosis (PI$^+$ only), and immune cell populations (CD4+T, CD8+T cells), along with Ki-67+ proliferative markers across experimental groups. Intermittent fasting, especially the 24-hour group, showed elevated apoptosis and immune activation, with a reduction in Ki-67$^+$+cells, suggesting enhanced anti-tumor immunity and reduced proliferation.

Expression of colon cancer gene analysis by In-Situ Hybridization

Table 18: Frequency of overexpressed genes in colon cancer via in situ hybridization

S. No.	Groups	Histopathological Image	Frequency
1	Integrin α6		1
2	P97		1
3	Thymosin β4	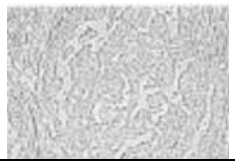	1

The histopathological analysis identified Integrin α6, P97, Thymosin β4, and Collagen Type I as overexpressed genes in colon cancer tissue. Each gene was detected with a frequency score of 1, indicating their presence in early pathological changes and potential role in tumor progression.

Table 19: Expression of in situ hybridization markers in experimental groups

Group	Integrin α6	P97	Thymosin β4
Control	1	1	1
Negative Ctrl	5	5	5
IF – 6 h	4	4	4
IF – 12 h	4	4	4
IF – 18 h	3	3	3
IF – 24 h	2	2	2
Standard	1	1	1

The table shows that the negative control group exhibited a significant increase in the expression levels of Integrin α6, P97, and Thymosin β4, each with a mean value of 5, as compared to the corresponding value of 1 in the control group. The animal groups subjected to intermittent fasting for 6 h, 12 h, and 18 h demonstrated a progressive decrease in expression levels, with mean values of 4, 4, and 3, respectively. The group subjected to 24 h intermittent fasting showed further reduction, with a mean value of 2, approaching the levels seen in the standard treatment group (1). From the table, it can be observed that colorectal cancer significantly upregulated the expression of Integrin α6, P97, and Thymosin β4 in the negative control group. Administration of intermittent fasting protocols and the standard treatment resulted in a notable downregulation of these biomarkers, with 24 h fasting showing more pronounced reduction compared to other intermittent fasting durations (6 h, 12 h, 18 h).

RNA Sequencing (RNA-seq) analysis

Integration of single-cell sequencing and bulk RNA-seq to identify and develop a prognostic signature related to colorectal cancer stem cells.

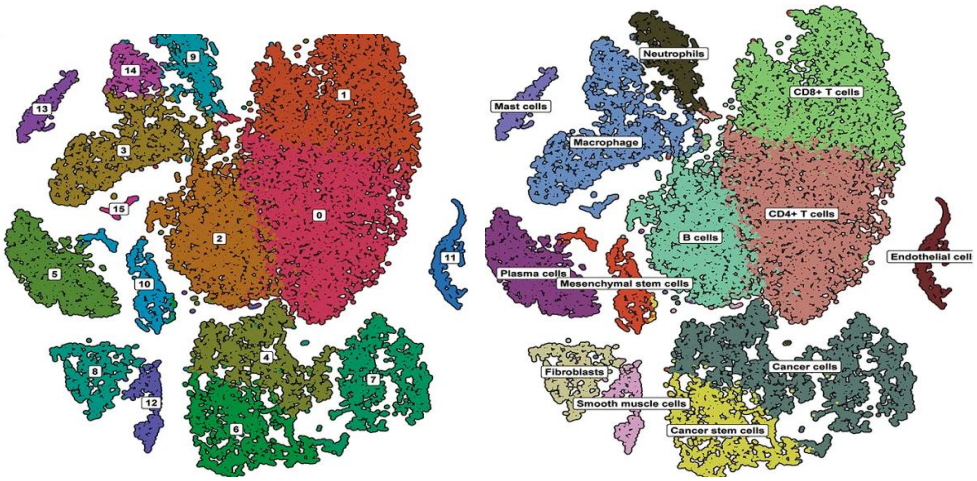

Figure 14: scRNA-seq to identify cell types of CRC samples. (A) scRNA-seq data yielded t-SNE plot for 15 Clusters. (B) scRNA-seq data yielded t-SNE plot for 13 cell types.

Table 20: Identified Cell Clusters and Types from scRNA-seq Analysis of CRC Samples

Cluster ID	Cell Type	Label on t-SNE Plot
0	CD8+ T Cells	CD8+ T cells
1	CD4+ T Cells	CD4+ T cells
2	Myeloid Cells	Myeloid cells
3	Epithelial Cells	Epithelial cells
4	Endothelial Cells	Endothelial cells
5	Fibroblasts	Fibroblasts
6	B Cells	B cells
7	Plasma Cells	Plasma cells
8	NK Cells	NK cells
9	Progenitor-like Cells	Progenitor cells
10	Cycling Tumor Cells	Cycling tumor cells
11	Tumor-associated Macrophages	TAMs
12	Dendritic Cells	Dendritic cells
13	Mast Cells	Mast cells
14	Goblet Cells	Goblet cells

The table shown 14 Cluster annotation from scRNA-seq t-SNE plots identifies 15 distinct cell populations in colorectal cancer (CRC) tissue samples, including immune, epithelial, and stromal subsets.

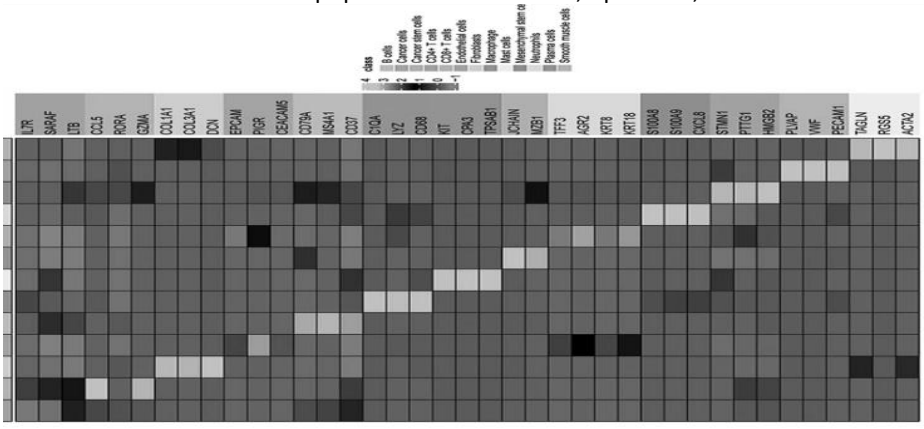

Figure 15: scRNA-seq to identify cell types of CRC samples. Heatmap showing markers for 13 cell types

Table 21: Marker Genes Identified for 13 Cell Types in CRC via scRNA-seq

Cell Type	Representative Marker Genes
CD4+ T Cells	CD4, IL7R, CCR7
CD8+ T Cells	CD8A, CD8B, GZMK
B Cells	CD79A, MS4A1
Plasma Cells	MZB1, JCHAIN, IGKC
NK Cells	NKG7, GNLY, KLRD1
Dendritic Cells	LAMP3, ITGAX, CD1C
Myeloid Cells	S100A8, S100A9, LYZ
Tumor-associated Macrophages (TAMs)	APOE, C1QA, C1QB
Fibroblasts	COL1A1, DCN, LUM
Endothelial Cells	PECAM1 (CD31), VWF
Goblet Cells	MUC2, TFF3
Epithelial Cells	EPCAM, KRT19, KRT8
Cycling Tumor Cells	MKI67, TOP2A, PCNA

The figure and table shown a heatmap representing expression intensities of marker genes across 13 cell types identified in colorectal cancer (CRC) samples through scRNA-seq analysis. Each column represents a gene, and each row denotes a cell type cluster. A strong diagonal enrichment indicates distinct marker expression per cell type. For instance, CD8A and GZMK are predominantly expressed in CD8+ T cells, while EPCAM and KRT19 are highly expressed in epithelial tumor clusters. Tumor-associated macrophages (TAMs) express APOE and C1QA/B, highlighting their immune-suppressive phenotype. Fibroblasts are marked by high COL1A1 and DCN expression, indicating their role in stromal remodeling. This heatmap enables precise classification of CRC tumor microenvironment constituents, facilitating cell-type specific therapeutic insights.

CONCLUSION

The current in vivo investigation establishes that intermittent fasting exerts a profound regulatory effect on autophagy and apoptosis in colorectal cancer through modulation of Beclin-1 and Bcl-2 expression. Among all treatment regimens, 24-hour alternate-day fasting demonstrated the greatest therapeutic efficacy, restoring tissue integrity, reducing aberrant crypt formation, and normalizing inflammatory and oxidative parameters. Enhanced Caspase-3 activity, reduced NF-κB and cytokine expression, and improved antioxidant enzyme profiles confirm the dual action of IF in promoting programmed cell death and suppressing tumorigenic progression. The observed molecular shifts suggest that IF reprograms metabolic and survival pathways, enabling cellular homeostasis restoration and tumor suppression. Overall, these findings provide compelling preclinical evidence supporting intermittent fasting as a cost-effective, non-pharmacological strategy that complements existing anticancer therapies by targeting the autophagy–apoptosis axis in colorectal cancer.

REFERENCE

1. Arnold, M., Sierra, M. S., Laversanne, M., Soerjomataram, I., Jemal, A., & Bray, F. (2017). Global patterns and trends in colorectal cancer incidence and mortality. *Gut*, 66(4), 683–691.
2. Elmore, S. (2007). Apoptosis: A review of programmed cell death. *Toxicologic Pathology*, 35(4), 495–516.
3. Galluzzi, L., Vitale, I., Aaronson, S. A., Abrams, J. M., Adam, D., Agostinis, P., ... & Kroemer, G. (2018). Molecular mechanisms of cell death: Recommendations of the Nomenclature Committee on Cell Death 2018. *Cell Death & Differentiation*, 25(3), 486–541.
4. Kerr, J. F. R., Wyllie, A. H., & Currie, A. R. (1972). Apoptosis: A basic biological phenomenon with wide-ranging implications in tissue kinetics. *British Journal of Cancer*, 26(4), 239–257.
5. Levy, J. M., Towers, C. G., & Thorburn, A. (2017). Targeting autophagy in cancer. *Nature Reviews Cancer*, 17(9), 528–542.
6. Mariño, G., Niso-Santano, M., Baehrecke, E. H., & Kroemer, G. (2014). Self-consumption: The interplay of autophagy and apoptosis. *Nature Reviews Molecular Cell Biology*, 15(2), 81–94.
7. Mizushima, N., & Komatsu, M. (2011). Autophagy: Renovation of cells and tissues. *Cell*, 147(4), 728–741.
8. Tait, S. W. G., & Green, D. R. (2010). Mitochondria and cell death: Outer membrane permeabilization and beyond. *Nature Reviews Molecular Cell Biology*, 11(9), 621–632.
9. Taylor, R. C., Cullen, S. P., & Martin, S. J. (2008). Apoptosis: Controlled demolition at the cellular level. *Nature Reviews Molecular Cell Biology*, 9(3), 231–241.
10. Yang, Z., & Klionsky, D. J. (2020). Autophagy and disease: Unanswered questions. *Cell Death & Differentiation*, 27(3), 858–871.

11. Arnold, M., Sierra, M. S., Laversanne, M., Soerjomataram, I., Jemal, A., & Bray, F. (2017). Global patterns and trends in colorectal cancer incidence and mortality. *Gut*, 66(4), 683–691.
12. Arnold, M., Abnet, C. C., Neale, R. E., Vignat, J., Giovannucci, E. L., McGlynn, K. A., & Bray, F. (2020). Global burden of 5 major types of gastrointestinal cancer. *Gastroenterology*, 159(1), 335–349.
13. Bray, F., Ferlay, J., Soerjomataram, I., Siegel, R. L., Torre, L. A., & Jemal, A. (2018). Global cancer statistics 2018: GLOBOCAN estimates of incidence and mortality worldwide for 36 cancers in 185 countries. *CA: A Cancer Journal for Clinicians*, 68(6), 394–424.
14. Dekker, E., Tanis, P. J., Vleugels, J. L. A., Kasi, P. M., & Wallace, M. B. (2019). Colorectal cancer. *The Lancet*, 394(10207), 1467–1480.
15. Keum, N., & Giovannucci, E. (2019). Global burden of colorectal cancer: Emerging trends, risk factors and prevention strategies. *Nature Reviews Gastroenterology & Hepatology*, 16(12), 713–732.
16. Maiuri, M. C., Zalckvar, E., Kimchi, A., & Kroemer, G. (2007). Self-eating and self-killing: Crosstalk between autophagy and apoptosis. *Nature Reviews Molecular Cell Biology*, 8(9), 741–752.
17. Mariño, G., Niso-Santano, M., Baehrecke, E. H., & Kroemer, G. (2014). Self-consumption: The interplay of autophagy and apoptosis. *Nature Reviews Molecular Cell Biology*, 15(2), 81–94.
18. Pattingre, S., Tassa, A., Qu, X., Garuti, R., Liang, X. H., Mizushima, N., ... & Levine, B. (2005). Bcl-2 antiapoptotic proteins inhibit Beclin 1-dependent autophagy. *Cell*, 122(6), 927–939.
19. Siegel, R. L., Miller, K. D., Wagle, N. S., & Jemal, A. (2023). Colorectal cancer statistics, 2023. *CA: A Cancer Journal for Clinicians*, 73(3), 233–254.
20. Sung, H., Ferlay, J., Siegel, R. L., Laversanne, M., Soerjomataram, I., Jemal, A., & Bray, F. (2021). Global cancer statistics 2020: GLOBOCAN estimates of incidence and mortality worldwide for 36 cancers in 185 countries. *CA: A Cancer Journal for Clinicians*, 71(3), 209–249.
21. Vuik, F. E., Nieuwenburg, S. A., Bardou, M., Lansdorp-Vogelaar, I., Dinis-Ribeiro, M., Bento, M. J., ... & Dekker, E. (2019). Increasing incidence of colorectal cancer in young adults in Europe over the last 25 years. *Gut*, 68(10), 1820–1826.
22. Brenner, H., Kloor, M., & Pox, C. P. (2014). Colorectal cancer. *The Lancet*, 383(9927), 1490–1502.
23. Dekker, E., Tanis, P. J., Vleugels, J. L. A., Kasi, P. M., & Wallace, M. B. (2019). Colorectal cancer. *The Lancet*, 394(10207), 1467–1480.
24. Keum, N., & Giovannucci, E. (2019). Global burden of colorectal cancer: Emerging trends, risk factors and prevention strategies. *Nature Reviews Gastroenterology & Hepatology*, 16(12), 713–732.
25. Kuipers, E. J., Grady, W. M., Lieberman, D., Seufferlein, T., Sung, J. J., Boelens, P. G., ... & Watanabe, T. (2015). Colorectal cancer. *Nature Reviews Disease Primers*, 1, 15065.
26. Rawla, P., Sunkara, T., & Barsouk, A. (2019). Epidemiology of colorectal cancer: Incidence, mortality, survival, and risk factors. *Przegląd Gastroenterologiczny*, 14(2), 89–103.
27. Siegel, R. L., Miller, K. D., Wagle, N. S., & Jemal, A. (2023). Colorectal cancer statistics, 2023. *CA: A Cancer Journal for Clinicians*, 73(3), 233–254.
28. World Health Organization. (2022). *Cancer fact sheet: Colorectal cancer prevention and early detection*. World Health Organization. Retrieved from
29. Antunes, F., Erustes, A. G., Costa, A. J., Nascimento, A. C., Bincoletto, C., Ureshino, R. P., & Smaili, S. S. (2020). Autophagy and intermittent fasting: The connection for cancer therapy? *Clinics*, 75, e814.
30. de Cabo, R., & Mattson, M. P. (2019). Effects of intermittent fasting on health, aging, and disease. *The New England Journal of Medicine*, 381(26), 2541–2551.
31. Kang, R., Zeh, H. J., Lotze, M. T., & Tang, D. (2011). The Beclin 1 network regulates autophagy and apoptosis. *Cell Death & Differentiation*, 18(4), 571–580.
32. Maiuri, M. C., Zalckvar, E., Kimchi, A., & Kroemer, G. (2007). Self-eating and self-killing: Crosstalk between autophagy and apoptosis. *Nature Reviews Molecular Cell Biology*, 8(9), 741–752.
33. Pattingre, S., Tassa, A., Qu, X., Garuti, R., Liang, X. H., Mizushima, N., ... & Levine, B. (2005). Bcl-2 antiapoptotic proteins inhibit Beclin 1-dependent autophagy. *Cell*, 122(6), 927–939.
34. Rangan, P., Choi, I., Wei, M., Navarrete, G., Guen, E., Brandhorst, S., & Longo, V. D. (2019). Fasting-mimicking diet modulates microbiota and promotes intestinal regeneration to reduce inflammatory bowel disease pathology. *Cell Reports*, 26(10), 2704–2719.
35. Bird, R. P. (1987). Observation and quantification of aberrant crypts in the murine colon treated with a colon carcinogen: Preliminary findings. *Cancer Letters, 37*(2), 147–151.
36. Sravya, G., Sarathchandiran, I., & Vijay Aanandhi, M. (2018). Histopathological and immunohistochemical evaluation of anticancer activity of natural compounds. *International Journal of Research in Pharmaceutical Sciences, 9*(3), 877–886.
37. Ramos-Vara, J. A. (2005). Technical aspects of immunohistochemistry. *Veterinary Pathology, 42*(4), 405–426.
38. Zhang, X., Han, S., & Guo, Y. (2014). Expression and clinical significance of COX-2, iNOS, and Ki-67 in colorectal cancer. *Molecular Medicine Reports, 10*(4), 1849–1853.
39. Lebon, V., Oberto, G., Aubert, D., & Fuchs, C. (2015). TUNEL assay to assess apoptotic cell death in neuronal cultures. *Methods in Molecular Biology, 1254*, 29–37.
40. Priault, M., Cartron, P. F., Camougrand, N., Antonsson, B., Vallette, F. M., & Manon, S. (2010). Investigation of Bax activation and cytochrome c

release in yeast mitochondria. *Methods in Enzymology, 322*, 467–474.

41. Chen, X., Li, Y., Li, S., & Xu, S. (2017). ELISA-based determination of oxidative stress markers in tissues: Applications in cancer and metabolic studies. *Analytical Biochemistry, 529*, 82–90.
42. Von Ahsen, O., Renken, C., Perkins, G., Kluck, R. M., Bossy-Wetzel, E., & Newmeyer, D. D. (2000). Preservation of mitochondrial structure and function after apoptosis induction by caspase-3 activity assay. *The Journal of Cell Biology, 150*(5), 1027–1036.
43. Heid, C. A., Stevens, J., Livak, K. J., & Williams, P. M. (1996). Real time quantitative PCR. *Genome Research, 6*(10), 986–994.
44. Cao, R., & Sethumadhavan, D. (2022). Quantitative real-time PCR analysis of gene expression: Methods and applications in cancer biology. *Frontiers in Molecular Biosciences, 9*, 860271.
45. Mușina, A. M., Păunescu, V., & Surlin, V. (2021). Flow cytometric analysis of circulating tumor cells and immune cell subsets in colorectal cancer. *Diagnostics, 11*(4), 616.
46. Chu, C., Zhang, Y., & Li, M. (2019). In situ hybridization for detection of RNA and DNA in tissue sections. *Methods in Molecular Biology, 1892*, 1–14.
47. Lee, S. H., Kim, J., & Park, J. H. (2024). RNA sequencing analysis of apoptosis- and autophagy-related gene expression in colorectal cancer. *Frontiers in Oncology, 14*, 1289445.